The Journal of the Astronautical Sciences, Vol. 54, Nos. 3 & 4, July–December 2006, pp. 567–582

Study of the Gravitational Capture in the Elliptical Restricted Three-Body Problem[1]

Antônio Fernando Bertachini de Almeida Prado[2] and Ernesto Vieira Neto[3]

Introduction

Gravitational capture is the phenomenon where a particle, coming from outside the sphere of influence of another body, may have its velocity relative to the celestial body reduced and it can even stay in orbit around it temporarily, using only gravitational forces. This happens due to the change of the two-body energy of the massless body from positive to negative relative to one of the primaries of the restricted three-body problem. The two-body energy is constant in the two-body problem, but not in the three-body problem, where this energy is not conserved due to the perturbation of the third body. The importance of this study is that the results can be used to decrease the fuel expenditure for a mission going from one of the primaries to the other, like an Earth-Moon mission. This is performed by applying an impulse to the spacecraft during the temporary capture to accomplish a permanent capture. The application of this phenomenon in spacecraft trajectories is recent in the literature. The first demonstration of this was in 1987 (Belbruno [1]). Further studies include Belbruno [2, 3]; Krish [4]; Krish, Belbruno, and Hollister [5]; Miller and Belbruno [6]; Belbruno and Miller [7, 8]. They all studied missions in the Earth-Moon system that use this technique to save fuel during the insertion of the spacecraft in its final orbit around the Moon. Another set of papers that made fundamental contributions in this field, also with the main objective of constructing real trajectories in the Earth-Moon system, are those of Yamakawa, Kawaguchi, Ishii, and Matsuo (see references [9]–[12]). The first real application of a ballistic capture transfer was made during an emergency in a Japanese spacecraft [13]. After that, some studies that consider the time required for this transfer appeared in the literature. Examples of this approach can be found in the papers by Vieira-Neto and Prado [14, 15]. The references related to the gravitational capture for the elliptic case, like Bailey [16, 17, 18] and Heppenheimer [19], do not use the variation of the two-body energy as done in this paper.

[1]Presented as paper AAS 05-475 at the AAS Malcolm D. Shuster Astronautics Symposium, State University of New York, Buffalo, New York, June 12–15, 2005.
[2]Instituto Nacional de Pesquisas Espaciais, São José dos Campos, SP, Brazil. E-mail: prado@dem.inpe.br.
[3]FEG-UNESP, Guaratinguetá-SP, Brazil. E-mail: ernesto@feg.unesp.br.

The Elliptic Restricted Three-Body Problem

The equations of motion for the spacecraft are assumed to be the ones valid for the well-known planar restricted elliptic three-body problem. The standard canonical system of units is used, which implies that:

1. The unit of distance is the semimajor axis of the orbit M_1 and M_2;
2. The angular velocity (ω) of the motion of M_1 and M_2 is assumed to be one;
3. The mass of the smaller primary (M_2) is given by $\mu = \dfrac{m_2}{m_1 + m_2}$ (where m_1 and m_2 are the real masses of M_1 and M_2, respectively) and the mass of M_1 is $(1 - \mu)$, to make the total mass of the system unitary;
4. The unit of time is defined such that the period of the motion of the two primaries is 2π;
5. The gravitational constant is one.

There are several systems that can be used to describe the elliptic restricted problem [20]. In this section the fixed (inertial) and the rotating-pulsating systems are described.

In the fixed system the origin is located in the barycenter of the two heavy masses M_1 and M_2. The horizontal axis is the line connecting M_1 and M_2 and the vertical axis is perpendicular to the horizontal axis. In this system the positions of M_1 and M_2 are

$$\bar{x}_1 = -\mu r \cos \nu \tag{1}$$

$$\bar{y}_1 = -\mu r \sin \nu \tag{2}$$

$$\bar{x}_2 = (1 - \mu) r \cos \nu \tag{3}$$

$$\bar{y}_2 = (1 - \mu) r \sin \nu \tag{4}$$

where r is the distance between the two primaries, given by $r = \dfrac{1 - e^2}{1 + e \cos \nu}$, and ν is the true anomaly of M_2. Then, in this system, the equations of motion of the massless particle are

$$\bar{x}'' = \frac{-(1 - \mu)(\bar{x} - \bar{x}_1)}{r_1^3} - \frac{\mu(\bar{x} - \bar{x}_2)}{r_2^3} \tag{5}$$

$$\bar{y}'' = \frac{-(1 - \mu)(\bar{y} - \bar{y}_1)}{r_1^3} - \frac{\mu(\bar{y} - \bar{y}_2)}{r_2^3} \tag{6}$$

where $''$ means the second derivative with respect to nondimensional time, r_1 and r_2 are the distances from M_1 and M_2, given by

$$r_1^2 = (\bar{x} - \bar{x}_1)^2 - (\bar{y} - \bar{y}_1)^2 \tag{7}$$

$$r_2^2 = (\bar{x} - \bar{x}_2)^2 - (\bar{y} - \bar{y}_2)^2 \tag{8}$$

Now the rotating-pulsating system of reference is introduced. In this system, the origin is again the center of mass of the two massive primaries. The horizontal axis (x) is the line that connects the two primaries. It rotates with a variable angular velocity in such a way that the two massive primaries are always in this axis. The vertical axis (y) is perpendicular to the x-axis. Besides the rotation, the system also

pulsates in such a way to keep the massive primaries in fixed positions. To achieve this situation, the unit of distances is multiplied by the instantaneous value of the distance between the two primaries (r). In a system like this one, the positions of the primaries are

$$x_1 = -\mu, x_2 = 1 - \mu, y_1 = y_2 = 0 \tag{9}$$

In this system, the equations of motion for the massless particle are

$$\ddot{x} - 2\dot{y} = \frac{r}{p}\left(x - (1-\mu)\frac{x - x_1}{r_1^3} - \mu\frac{x - x_2}{r_2^3}\right) \tag{10}$$

$$\ddot{y} + 2\dot{x} = \frac{r}{p}\left(y - (1-\mu)\frac{y}{r_1^3} - \mu\frac{y}{r_2^3}\right) \tag{11}$$

and there is also an equation that relates time and the true anomaly of the primaries

$$\dot{t} = \frac{r^2}{p^{1/2}} \tag{12}$$

where the over dot means derivative with respect to the true anomaly of the primaries and p is the semi-lactus rectum of the ellipse.

The equations that relate one system to another are

$$\bar{x} = rx\cos\nu - ry\sin\nu \tag{13}$$

$$\bar{y} = rx\sin\nu + ry\cos\nu \tag{14}$$

$$x = (\bar{x}\cos\nu + \bar{y}\sin\nu)/r \tag{15}$$

$$y = (\bar{y}\cos\nu - \bar{x}\sin\nu)/r \tag{16}$$

for the positions and

$$\bar{x}' = x'r\cos\nu - y'r\sin\nu - \frac{x(1-e^2)\sin\nu}{(1+e\cos\nu)^2} - \frac{y(1-e^2)(e+\cos\nu)}{(1+e\cos\nu)^2} \tag{17}$$

$$\bar{y}' = x'r\sin\nu + y'r\cos\nu - \frac{y(1-e^2)\sin\nu}{(1+e\cos\nu)^2} + \frac{x(1-e^2)(e+\cos\nu)}{(1+e\cos\nu)^2} \tag{18}$$

$$x' = \frac{\bar{x}'\cos\nu}{r} + \frac{\bar{y}'\sin\nu}{r} - \frac{\bar{x}(\sin\nu + e\sin 2\nu)}{1-e^2} + \frac{\bar{y}(\cos\nu + 2e\cos^2\nu - e)}{1-e^2} \tag{19}$$

$$y' = \frac{\bar{y}'\cos\nu}{r} - \frac{\bar{x}'\sin\nu}{r} - \frac{\bar{y}(\sin\nu + e\sin 2\nu)}{1-e^2} - \frac{\bar{x}(\cos\nu + 2e\cos^2\nu - e)}{1-e^2} \tag{20}$$

for the velocities, where $p = 1 - e^2$ and $r = \dfrac{1-e^2}{1+e\cos\nu}$.

The Gravitational Capture

To define the gravitational capture it is necessary to use a few basic concepts from the two-body celestial mechanics. Those concepts are

a. Closed orbit: a spacecraft in an orbit around a central body is in a closed orbit if its velocity is not large enough to escape from the central body. It remains always inside a sphere centered in the central body;

b. Open orbit: a spacecraft in an orbit around a central body is in an open orbit if its velocity is large enough to escape from the central body. In this case, the spacecraft can go to infinity, no matter what is its initial position.

To identify the type of orbit of the spacecraft it is possible to use the definition of the two-body energy (E) of a massless particle orbiting a central body. The equation is $E = \frac{V^2}{2} - \frac{\mu}{r}$, where V is the velocity of the spacecraft relative to the central body, μ is the gravitational parameter of the central body and r is the distance between the spacecraft and the central body.

With this definition it is possible to say that the spacecraft is in an open orbit if its energy is positive and that it is in a closed orbit if its energy is negative. In the two-body problem this energy remains constant and it is necessary to apply an external force to change it. This energy is no longer constant in the restricted three-body problem. Then, for some initial conditions, a spacecraft can alternate the sign of its energy from positive to negative or from negative to positive. When the variation is from positive to negative the maneuver is called a "gravitational capture," to emphasize that the spacecraft was captured by gravitational forces only, with no use of an external force, like the thrust of an engine. The opposite situation, when the energy changes from negative to positive is called a "gravitational escape." In the restricted three-body problem there is no permanent gravitational capture. If the energy changes from positive to negative, it will change back to positive in the future. The mechanism of this capture is very well explained in all the references cited in this paper.

Assumptions to Study This Problem

To study this problem, several assumptions are made. They are

1. The true anomaly (γ) of the secondary body is the parameter used to study the importance of the eccentricity in the problem (see Fig. 1);
2. The motion is planar;
3. The starting point of each trajectory is 100 km from the Moon's surface ($\approx$0.0045 in canonical units from the center of the smallest primary). The angle α, from the line joining the two primaries, shown in Fig. 1, is used to compute the initial position;

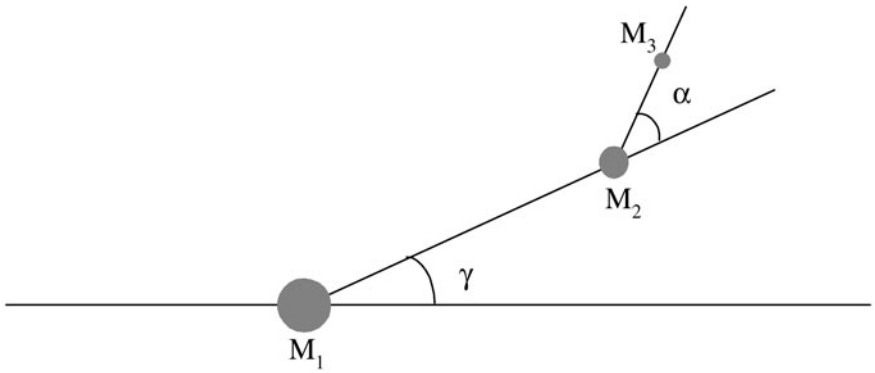

FIG. 1. Configuration of the Bodies at $t = 0$ in the Elliptical Restricted Three-Body Problem.

4. The magnitude of the initial velocity is calculated from a given value of $C_3 = v^2 - 2\mu/r_2$, where v is the velocity of the massless body relative to the smallest primary. Here, and in several other points of the present paper, a transformation between the velocity with respect to the primaries and the velocity given by the rotating-pulsating system is required. To perform this task, equations (17) to (20) are used for the conversion between the velocities in the inertial and in the rotating-pulsating system and, then, a direct vector subtraction can give the velocity with respect to the primaries, since the inertial velocities of the primaries are known from the elliptic theory of orbits. The direction of the velocity is assumed to be perpendicular to the line joining the smallest primary to the massless body in a counterclockwise direction;
5. The escape occurs when the spacecraft reaches a distance of 100.000 km (0.26 in canonical units) from the center of the smallest primary in a time shorter than 50 days ($\approx$12 in canonical units) [11];
6. For each initial condition, the trajectory was numerically integrated backward in time. Every escape in backward time corresponds to a gravitational capture in a forward time.

Some Results

As an example of the calculations performed in the present paper, the results for the cases where the eccentricity of the primaries is kept constant and the true anomaly assumes the values 0°, 90°, 180°, 270° is shown. The Earth-Moon system is used, so the eccentricity is fixed in the value 0.0549. Figure 2 shows the numerical results in plots where the radial variable is the magnitude of C_3 and the angular variable is the angle α. Figure 3 shows the circular case, for comparison. The savings are greater where the secondary body is at periapse ($\gamma = 0°$), what is expected, since the smaller distance between the two primaries increases the effect of the third body (the main cause of the savings). It is also clear the regions of maximum and minimum savings. When the Moon is at the perigee, the differences between the circular and elliptic models are very small. These differences are increased for the positions of α around 10°–20° and 340°–350°. At those points the value of C_3 goes up to -0.22 canonical units for the elliptic case, while for the circular case it stays at -0.21. Regions around 70°–80° are also of interest.

The fact that the eccentric dynamics allows larger savings when compared to the circular one for some points is an important result. The eccentric dynamics better represent the reality, and it is also possible to use it to obtain an extra savings, in the order of 4.76% (from -0.21 to -0.22 canonical units). Better models for the dynamics, that include more forces, could lead to even larger savings.

The jump close to $\alpha = 60°$ shown in Fig. 3 also appeared in reference [11]. It is located between $\alpha = 57.5°$ and 57.6°. There are many other discontinuities similar to this one in other plots. To understand the reason for that, a plot of two trajectories is made in Fig. 4, both with $C_3 = -0.16$, but using $\alpha = 57.5°$ for the first one and $\alpha = 57.6°$ for the second one. It is clear that, changing only 0.1° in α, one trajectory can leave the sphere of influence of the Moon, while the other one collides with the Moon. This fact can be easily noted in Fig. 4, because both trajectories initially escape from the Moon, then they make a return to pass close to the Moon again. At this point, the first trajectory follows its way going far way from the Moon, while the second trajectory collides with the Moon. This fact causes the discontinuities shown in the plots.

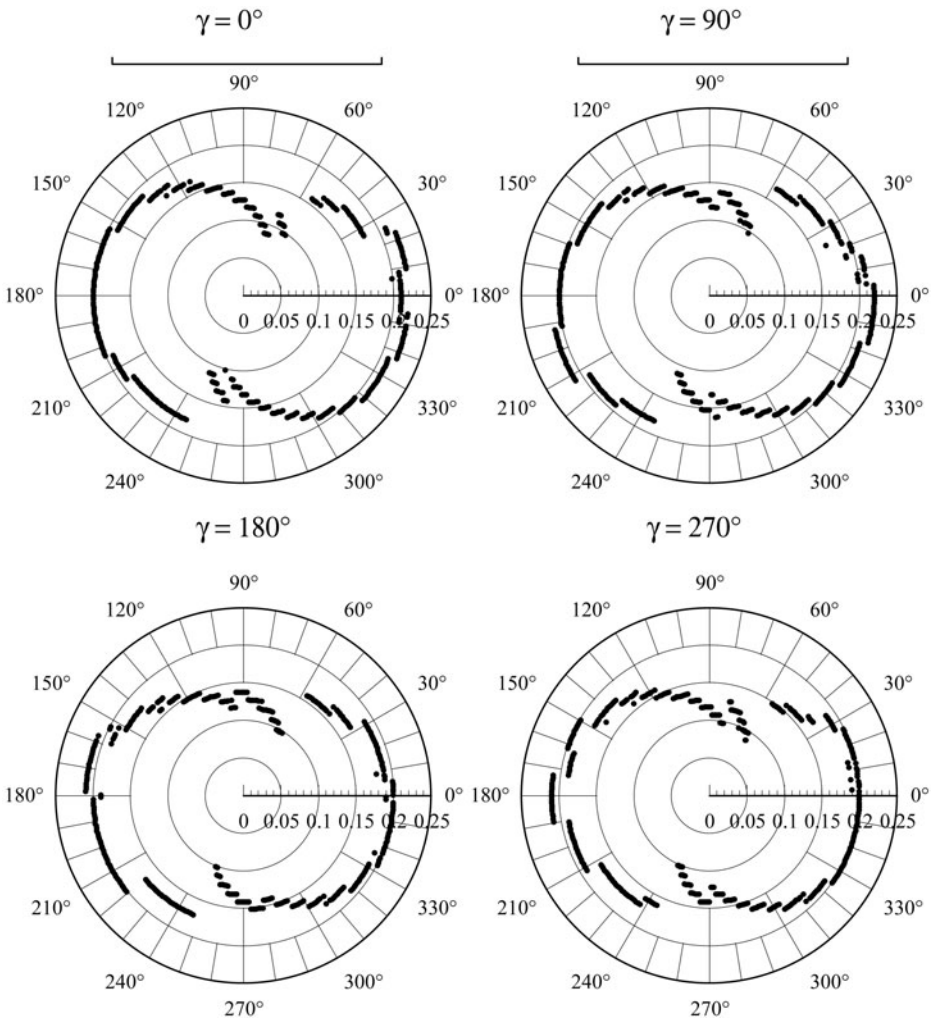

FIG. 2. Minimum C_3 for the Earth-Moon System ($e = 0.0549$) with $\gamma = 0°, 90°, 180°, 270°$.

To study in more detail the effect of the initial true anomaly (angle γ) in the savings of energy, Fig. 5 shows the variation of C_3 with γ, when α is kept fixed.

This figure shows that the conditions in α are more important than in γ for the values of the eccentricities simulated. When the true anomaly changes, keeping α constant, the minimum energy is almost the same. In the case where $\alpha = 0°$, the perilune are at the opposite side of the Earth, and this geometry allows the minimum values of C_3.

For $\alpha = 180°$ the minimum energy does not reach levels of energy as low as for the case $\alpha = 0°$, but it shows regularity and levels of two-body energy lower than in the cases $\alpha = 90°$ and $\alpha = 270°$. In more realistic cases, it is possible to make the transfers when $\gamma = 0°$, since there are disadvantages in terms of the potential savings in the cases $\gamma \neq 0°$.

Then, some hypothetical systems are studied, with the goal of having more details about the effect of the eccentricity in this problem. Figure 6 shows results

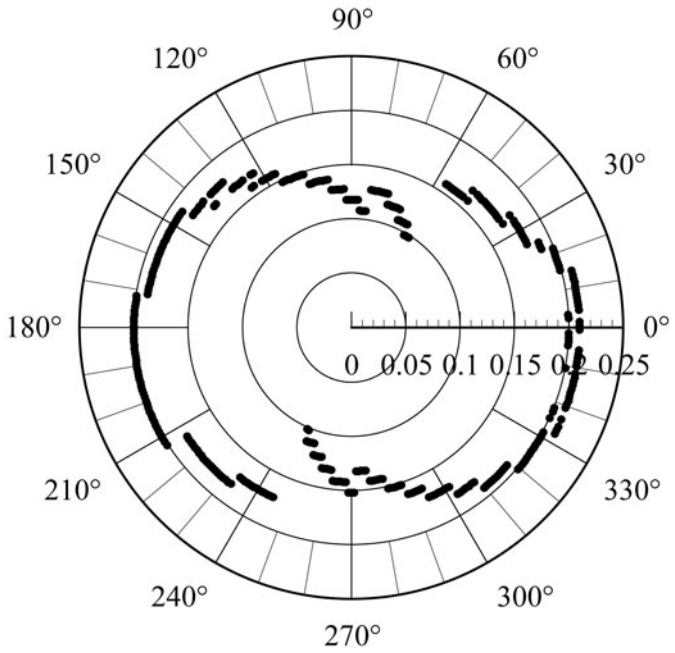

FIG. 3. Minimum C_3 for the Earth-Moon System Assuming the Circular Case.

when $\mu = 0.01$, and the eccentricities of the primaries are 0.0, 0.2, 0.4, and 0.8. The true anomaly assumes the values 0°, 90°, 180°, 270° for every value of the eccentricity. In this figure, the magnitude of C_3 in canonical units is the radial variable and the angle α is the angular variable. The eccentricity is 0.0 for the first plot, 0.2 for the second, 0.4 for the third, and 0.8 for the fourth one. It is clear that the lowest level of energy appears when the smaller primary is at periapse ($\gamma = 0°$) and the worst results appear when it is at the apoapses ($\gamma = 180°$). When $\gamma = 90°$ and $\gamma = 270°$ there are intermediate results. This is expected, because the smaller

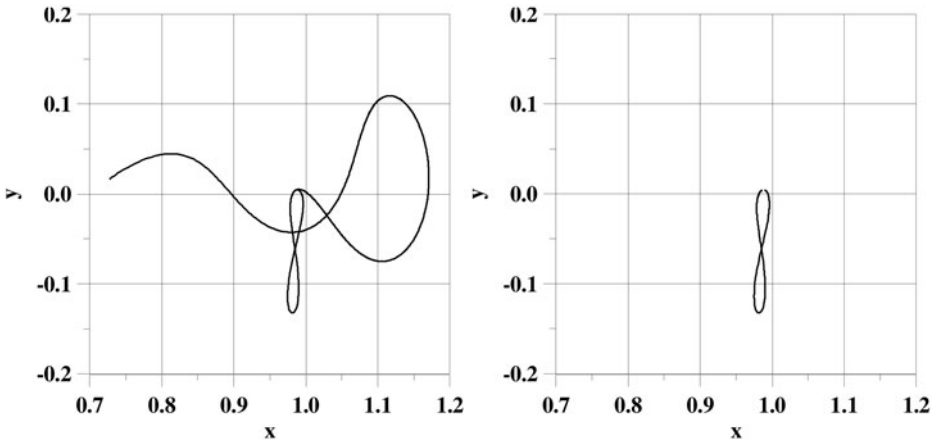

FIG. 4. Discontinuities for the case $C_3 = -0.16$. At the left, the trajectory for $\alpha = 57.5°$, where there is an escape. At the right, the trajectory for $\alpha = 57.6°$, where there is a collision.

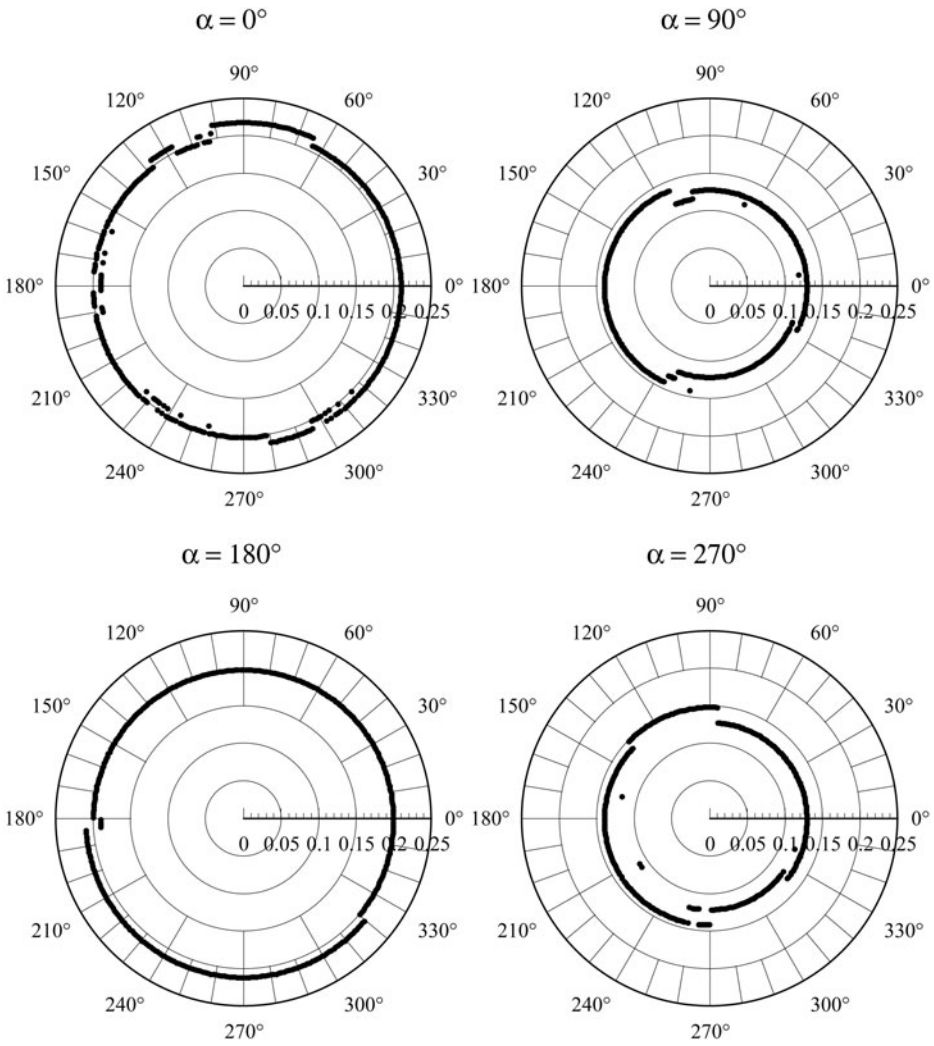

FIG. 5. Minimum Value of C_3 vs. γ for α Constant.

distance between the primaries increases the third body perturbation, which is the main cause of the reduction of energy. From those results it is also possible to conclude that, by increasing the eccentricity, there is an increase in the differences of the level of energy for the families $\gamma = 0°$, 90°, 180°, 270° (those families appear with more difference from each other). It is also possible to conclude that the increase of the eccentricity increases the levels of savings to increase. The radial scale goes from 0.2 (for $e = 0.0$) to 0.8 (for $e = 0.8$). Those figures also show the importance of the choice of the angle α. The differences in the magnitude of C_3 obtained by different values of this parameter are very large.

Effects of the Eccentricity in the Time Required for the Capture

For this analysis, the energy $C_3 = -0.14$ was selected and fixed. Two situations were studied. In the first one the eccentricity was fixed at 0.4 and the true anomaly varied from 0° to 270° in steps of 90°. These results are shown in Fig. 7. In this figure

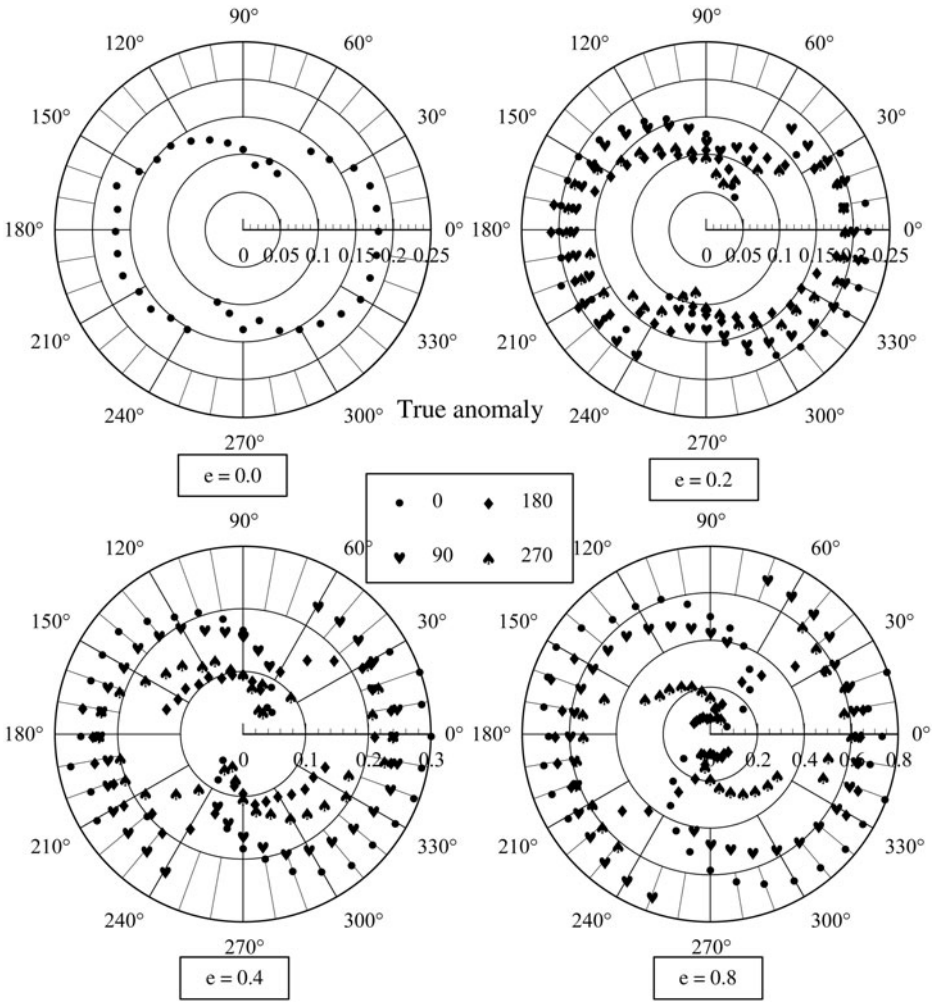

FIG. 6. Minimum C_3 for $\mu = 0.01$ and Several Values of the Eccentricity.

the radial variable is the time of capture in canonical units and the angular variable is the angle α. There are four positions for the Moon, where $\gamma = 0^\circ$ is the position closest to the Earth and $\gamma = 180^\circ$ is the position with more distance from the Earth. Each point corresponds to one trajectory.

After that, the true anomaly was fixed at 0° and the eccentricity was varied to assume the values 0.0, 0.2, 0.4, and 0.8. These results are shown in Fig. 8. Those systems of primaries are similar to the Earth-Moon system, with the eccentricities increased to emphasize the results.

The plots show the existence of two families of trajectories. There are large variations in the time required for the capture, depending on the initial value of the angle α. This fact shows the importance of this study, because you can get shorter times for the transfer for a fixed value of the energy savings.

Looking at the plots for $\gamma = 0^\circ$ and $\gamma = 90^\circ$ in Fig. 7, the change in the results are small, because the majority of the captures have a time smaller than two canonical units. Looking at the case $\gamma = 180^\circ$, it is possible to see larger changes in the

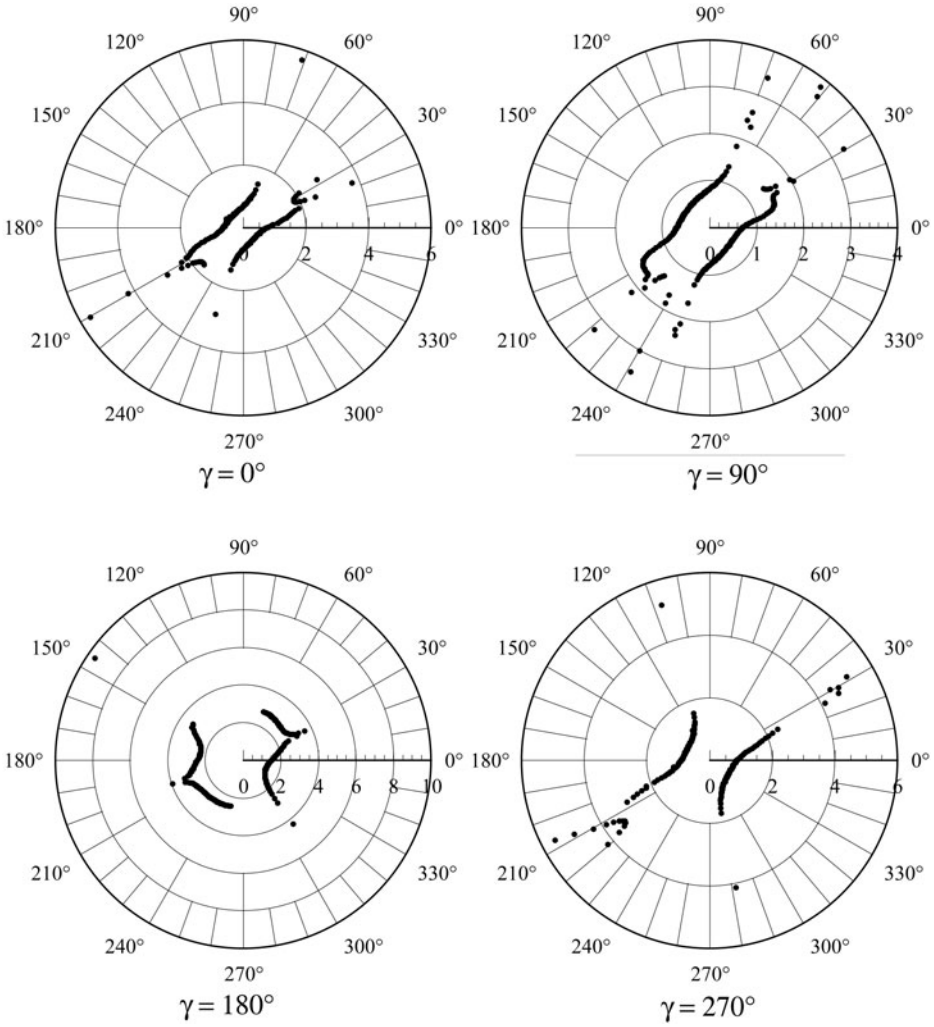

FIG. 7. Times for the Capture for Eccentricity of 0.4.

plots. Two new families of trajectories appear and the majority of them have times of capture between two and four canonical units of time. The largest distance between the two primaries in this geometry reduces the gravitational perturbation and increases the time to complete the capture. The results for $\gamma = 270°$ shows the return of the two characteristic families. But, larger values for the time of capture, when compared to the case $\gamma = 0°$, still appear and the number of trajectories that do not belong to the family increases.

Figure 8 shows the effect of the eccentricity in the time for the capture when $\gamma = 0°$ and the eccentricity is varied. In this figure the radial variable is the time of capture in canonical units and the angular variable in the angle α. Every point represents one trajectory. The characteristic of the problem of having two families is still valid here, this time for all the plots showed.

Those studies show that there is a measurable effect from increasing the eccentricity for a fixed value of the true anomaly. In general, there is a tendency to

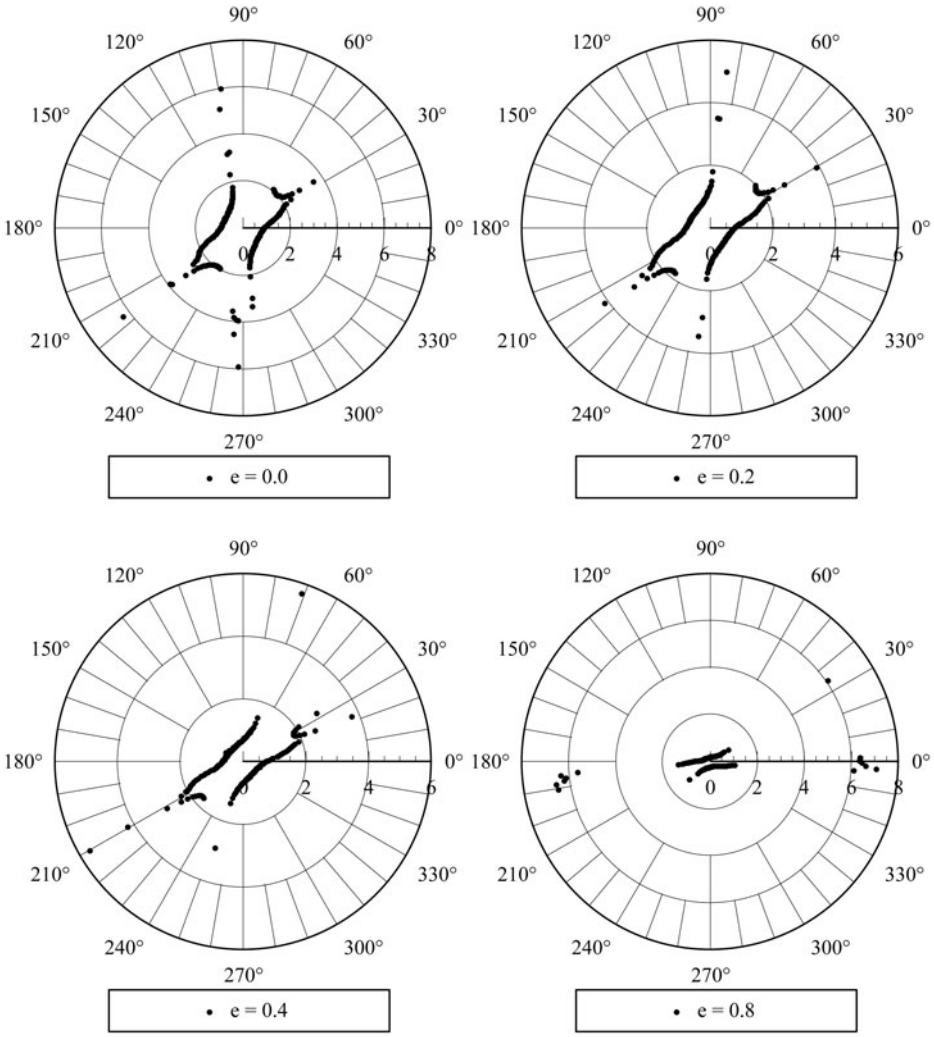

FIG. 8. Times for the Capture for $\gamma = 0°$.

reduce the time of capture with the increase of the eccentricity. This is also explained by the reduction of the distance between the primaries, since the positions studied are held constant at the periapses. Strong effects appear for large values of the eccentricity (like when $e = 0.8$), where the two families rotate in the clockwise direction, staying almost horizontal. This means that the value of α that allows minimum and maximum times of capture changes. These results can be used in optimization problems, like the ones shown below.

Optimization Problems

Several optimization problems can be solved using the results available in this research. Two of them are shown below.

Problem 1: Suppose that it is necessary to build a trajectory that ends in gravitational capture in a given system of primaries and for a fixed value of r_p. Assuming that $\mu = 0.0121506683$ (Earth-Moon system), it is desired that this trajectory has

the minimum possible time of flight, but with $C_3 = -0.14$ and $r_p = 0.004781477$. Figures 7 and 8 are used to solve this problem. This problem is solved for the eccentricities $e = 0.0, 0.2, 0.4$, and 0.8. The values for the true anomaly are $\gamma = 0°$, 90°, 180°, and 270°. The results are shown in Table 1. It includes the angle α and the time of capture. The savings in ΔV obtained is 0.031296 canonical units (0.032016 km/s) for all the cases, since C_3 is constant.

The results are in agreement with the general rule that says that, when the primaries are closer, the perturbation is larger and the time for the capture is smaller. For a fixed value of the eccentricity, the times are smaller for $\gamma = 0°$ and larger for $\gamma = 180°$. For a fixed value of the true anomaly, the time decreases with the increase of the eccentricity for $\gamma = 0°$ and it increases when $\gamma = 180°$. This means that the differences between the times of capture for different locations of the primaries increase with the eccentricity. The general conclusion is that, taking into account the effects of the eccentricity of the primaries, it is possible to design a trajectory that has the minimum time of capture. The regions of values of α does not change much, and the solutions are around $\alpha = 300° \pm 30°$. Figure 9 shows the trajectory of a space vehicle for the circular solution, as seen in the rotating frame.

This type of problem can be solved for different values of μ, r_p, C_3, etc. Similar problems with more degrees of freedom (like free r_p) can also be solved with the same technique.

Problem 2: Another variant of optimization problems that can be solved with the data shown here, is the problem of searching a gravitational capture trajectory that has a maximum savings subject to constraints in time, like a maximum time allowed for the maneuver. Figures 7 and 8 are also used to solve this problem. Assume that the Earth-Moon system is used and the value of $r_p = 0.004781477$ is required, together with the time limit of 0.8 canonical units of time for the maneuver. Again, four possibilities for the eccentricities and for the true anomaly are used. Table 2 shows the results. Compared with the circular solution, it is clear that for a fixed value of the eccentricity, C_3 reaches a minimum for $\gamma = 0°$ and a maximum for $\gamma = 180°$.

Then, the maximum savings for a problem with an upper limit of time is reached for the position $\gamma = 0°$. It is also noted that C_3 decreases with the increase of the eccentricity for $\gamma = 0°$ and it increases when $\gamma = 180°$.

TABLE 1. Solutions for Problem 1

e/γ	0°	90°	180°	270°
0	$\alpha = 338°$	—	—	—
	$t = 0.7482$	—	—	—
0.2	$\alpha = 311°$	335°	333°	331°
	$t = 0.6033$	0.6576	0.9452	0.7656
0.4	$\alpha = 325°$	312°	354°	330°
	$t = 0.4556$	0.5402	1.3657	0.7016
0.8	$\alpha = 292°$	281°	315°	330°
	$t = 0.1735$	0.1797	2.6443	0.3882

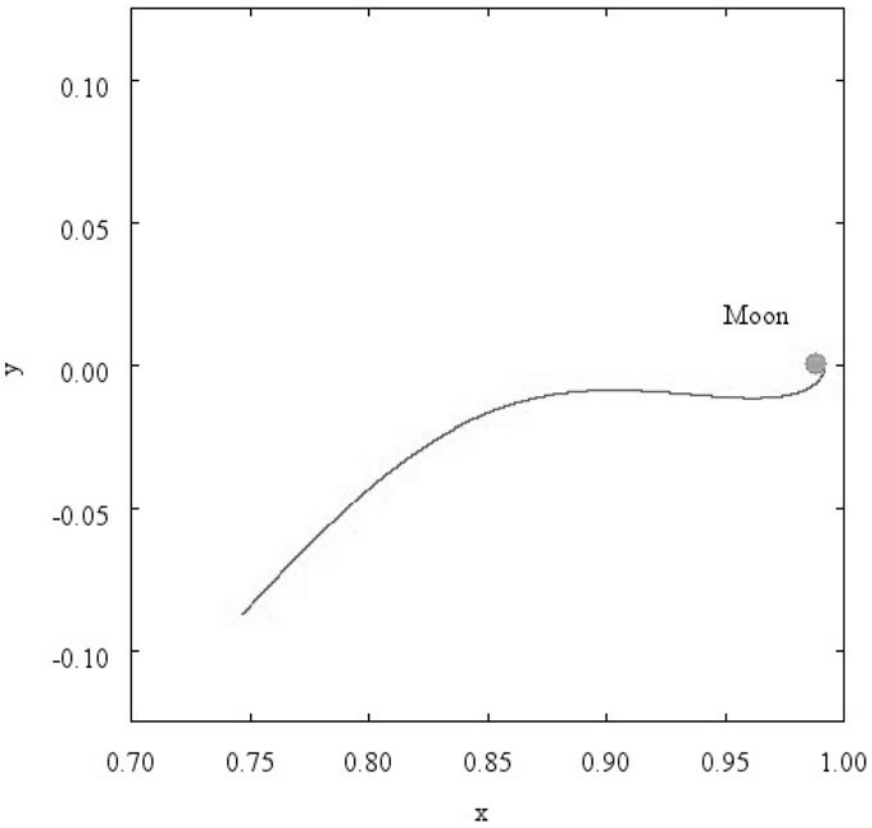

FIG. 9. Trajectory of Problem 1 (Canonical Units).

Then, the differences in energy for several final conditions of a specific trajectory increase with the increase of the eccentricity of this trajectory. The general conclusion is that, when taking into account the eccentricity of the primaries, it is possible to design a maneuver with maximum savings for a given time limit for the capture. The region of α that solves this problem is around $330° \pm 15°$. Figure 10 shows the trajectory of a spacecraft for the solution of the circular case, as seen

TABLE 2. Solutions for Problem 2

e/γ	0°	90°	180°	270°
0	$C_3 = -0.15$ $\alpha = 328°$	— —	— —	— —
0.2	$C_3 = -0.19$ $\alpha = 338°$	−0.17 321°	−0.11 346°	−0.14 331°
0.4	$C_3 = -0.28$ $\alpha = 328°$	−0.24 342°	−0.09 328°	−0.16 330°
0.8	$C_3 = -0.85$ $\alpha = 328°$	−0.71 333°	−0.07 346°	−0.34 330°

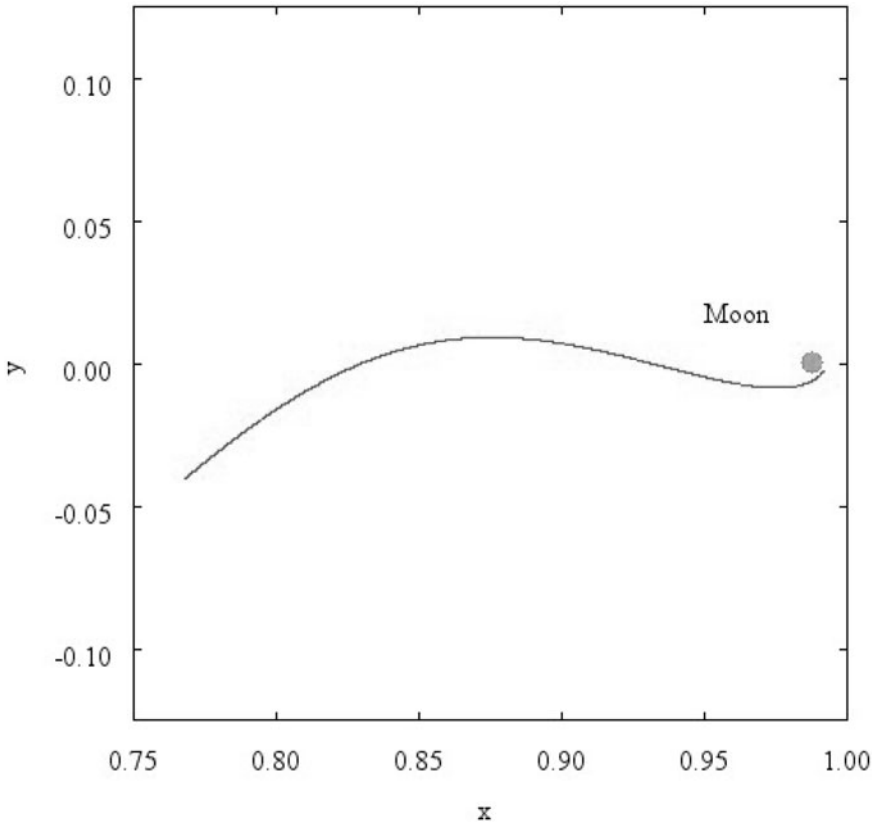

FIG. 10. Trajectory for Problem 2 (Canonical Units).

from the rotating system. Solutions for other cases can be obtained by solving a particular problem or interpolating the tables available.

Conclusions

A numerical algorithm was developed to study the problem of gravitational capture in the elliptical restricted three-body problem. The effect of the true anomaly for a fixed eccentricity and the effect of the eccentricity for a fixed true anomaly were studied.

From the results available, it is possible to conclude that the elliptic restricted three-body problem has some differences in the results, when compared with the circular case. These differences can be used in real missions to obtain some extra savings in fuel or in time for the maneuver. Figure 6 showed the locations and the magnitude of the differences between the two mathematical models and can be used to find optimal points for the maneuver.

The simulations made in this paper also explained the reason of some important discontinuities shown in the plots of minimum energy reached by the gravitational capture.

The main effect of the eccentricity is to decrease the two-body energy. Another important effect is that, if C_3 is held fixed, the time for the capture is reduced when the eccentricity is increased.

Regarding the true anomaly, the periapsis ($\gamma = 0°$) is the best location for the gravitational capture because it has the larger savings in terms of energy and the smaller times of capture.

The results showed in this paper also allow the formulation and solution of several practical problems involving optimization of parameters. Two examples were proposed and solved: 1) to find a trajectory that has a fixed energy and the minimum time of capture and; 2) to find one trajectory that has the minimum energy with a limit time for the capture. Both solutions were shown in details.

Acknowledgments

The author is grateful to the Foundation to Support Research in the São Paulo State (FAPESP) for the research grant received under Contract 03/03262-4 and to CNPq (National Council for Scientific and Technological Development)—Brazil for the contract 300828/2003-9.

References

[1] BELBRUNO, E. A. "Lunar Capture Orbits, a Method of Constructing Earth Moon Trajectories and the Lunar Gas Mission," presented as paper AIAA-87-1054 at the 19th AIAA/DGLR/JSASS International Electric Propulsion Conference, Colorado Springs, Colorado, May 1987.

[2] BELBRUNO, E. A. "Examples of the Nonlinear Dynamics of Ballistic Capture and Escape in the Earth-Moon System," presented as paper AIAA-90-2896 at the AIAA Astrodynamics Conference, Portland, Oregon, August 20–22, 1990.

[3] BELBRUNO, E. A. "Ballistic Lunar Capture Transfer Using the Fuzzy Boundary and Solar Perturbations: a Survey," *Proceedings for the International Congress of SETI Sail and Astrodynamics,* Turin, Italy, 1992.

[4] KRISH, V. *An Investigation into Critical Aspects of a New Form of Low Energy Lunar Transfer, the Belbruno-Miller Trajectories,* Master's Dissertation, Massachusetts Institute of Technology, Cambridge, MA, Dec. 1991.

[5] KRISH, V., BELBRUNO, E. A., and HOLLISTER, W. M. "An Investigation Into Critical Aspects of a New Form of Low Energy Lunar Transfer, the Belbruno-Miller Trajectories," presented as paper AIAA 92-4581-CP at the AIAA/AAS Astrodynamics Conference, Hilton Head Island, SC, August 10–12, 1992.

[6] MILLER, J. K. and BELBRUNO, E. A. "A Method for the Construction of a Lunar Transfer Trajectory Using Ballistic Capture," presented as paper AAS-91-100 at the AAS/AIAA Space Flight Mechanics Meeting, Houston, Texas, February 11–13, 1991.

[7] BELBRUNO, E. A. and MILLER, J. K. "A Ballistic Lunar Capture for the Lunar Observer," Jet Propulsion Laboratory, JPL IOM 312/90.4-1752, Internal Document, Pasadena, CA, Aug., 1990.

[8] BELBRUNO, E. A. and MILLER, J. K. "Sun-Perturbed Earth-to-Moon Transfers with Ballistic Capture," *Journal of Guidance, Control and Dynamics,* Vol. 16, No. 4, 1993, pp. 770–775.

[9] YAMAKAWA, H., KAWAGUCHI, J., ISHII, N., and MATSUO, H. "A Numerical Study of Gravitational Capture Orbit in Earth-Moon System," presented as paper AAS 92-186 at the AAS/AIAA Space Flight Mechanics Meeting, Colorado Springs, Colorado, February 24–26,1992.

[10] YAMAKAWA, H., KAWAGUCHI, J., ISHII, N., and MATSUO, H. "On Earth-Moon Transfer Trajectory with Gravitational Capture," presented as paper AAS 93-633 at the AAS/AIAA Astrodynamics Specialist Conference, Victoria, Canada, August 16–19, 1993.

[11] YAMAKAWA, H. *On Earth-Moon Transfer Trajectory with Gravitational Capture,* Ph.D. Dissertation, University of Tokyo, 1992.

[12] KAWAGUCHI, J. "On the Weak Stability Boundary Utilization and its Characteristics," presented as paper AAS 00-176 at the AAS/AIAA Space Flight Mechanics Meeting, Clearwater, Florida, January 23–26, 2000.

[13] BELBRUNO, E. A. and MILLER, J. K. "A Ballistic Lunar Capture Trajectory for Japanese Spacecraft Hiten," Jet Propulsion Lab., JPL IOM 312/90.4-1731, Internal Document, Pasadena, CA, June 1990.

[14] VIEIRA NETO, E. and PRADO, A. F. B. A. "A Study of the Gravitational Capture in the Restricted-Problem," *Proceedings of the International Symposium on Space Dynamics,* Toulouse, France, June 19–23, 1995, pp. 613–622.
[15] VIEIRA NETO, E. and PRADO, A. F. B. A. "Time-of-Flight Analyses for the Gravitational Capture Maneuver," *Journal of Guidance, Control and Dynamics,* Vol. 21, No. 1, 1998, pp. 122–126.
[16] BAILEY, J. M. "Jupiter: Its Captured Satellites," *Science,* Vol. 173, 1971, pp. 812–813.
[17] BAILEY, J. M. "Origin of the Outer Satellites of Jupiter," *Journal of Geophysical Research,* Vol. 76, No. 32, 1971, pp. 7827–7832.
[18] BAILEY, J. M. "Studies on Planetary Satellites: Satellite Capture in the Three-Body Elliptical Problem," *The Astronomical Journal,* Vol. 77, No. 2, 1972, pp. 177–182.
[19] HEPPENHEIMER, T. A. "On the Presumed Capture Origin of Jupiter's Outer Satellites," *Icarus,* Vol. 24, 1975, pp. 172–180.
[20] SZEBEHELY, V. G. *Theory of Orbits,* Academic Press, New York, 1967.